2023 International Conference on Unmanned Aircraft Systems (ICUAS)
June 6-9, 2023 | Lazarski University, Warsaw, Poland

A Fully-Actuated Drone with Rotating Seesaws

Dolev Yecheskel[1] and Shai Arogeti[2]

2023 International Conference on Unmanned Aircraft Systems (ICUAS) | 979-8-3503-1037-5/23/$31.00 ©2023 IEEE | DOI: 10.1109/ICUAS57906.2023.10155984

***Abstract*— Standard drones are generally underactuated systems, an attribute that limits their maneuvering ability. This limitation is because of the inherent coupling between the total thrust direction and the angular state of the drone body. To decouple these quantities, we suggest using seesaws, which allow controlling the thrust direction independently. Unlike other structures based on additional actuators to tilt the thrust, our solution is not based on any extra actuator that does not contribute to the lifting force. The presented configuration is an octocopter with eight propellers and four seesaws. These results extend a former suggested structure based on a single seesaw.**

I. Introduction

Due to its simple structure and ease of operation, the quadrotor is one of the most popular drones. The standard quadrotor has four propellers that are fixed to its frame. If a larger thrust is needed, more propellers are typically added to the frame; common structures are the hexacopter, with six propellers, and the octocopter, with eight propellers. Hexacopters and octocopters are utilized to carry loads that are too heavy for small quadrotors. Because of their extra propellers (more than the minimum needed for a controlled motion in space), they allow for improved survivability due to the potential to implement active fault-tolerant algorithms.

In all standard drones (quadrotors, hexacopters, octocopters, etc.), all thrust forces are parallel, and their direction is fixed with respect to the frame (usually pointing upwards). Hence any maneuver that is not idle hovering, requires tilting the drone's body in order to tilt the driving thrust. For most drone applications, this limitation is not an obstacle, because the drone task is just moving from point to point with no demand on its orientation. For some applications (such as aerial photography) the drone is carrying a tool (e.g., a video camera) and the orientation of the tool is important for its functionality. In these cases, the problem can be solved by using active gimbals that decouple the angular motion of the drone from that of the tool. However, these gimbals put extra weight and are typically expensive.

An underactuated system is a system in which the inputs cannot control all state variables independently. A standard drone is a good example of that because no matter the number of propellers, if they are all parallel and fixed in the frame, only four degrees of freedom can be controlled independently. Usually, these are the three position coordinates and the heading. Many alternative configurations were suggested in the scientific literature to improve the drone maneuvering ability. They can generally be divided into two groups ([1]); propellers with fixed tilting ([2][3],[4]) and propellers with active tilting ([5],[6],[7]). The application of control surfaces in a fully actuated quadrotor has been presented in [8]. We suggest an alternative approach based on the use of seesaws. The advantage is that no actuators are added to the platform that do not contribute lift force.

In [9], we suggested a hexacopter with a single seesaw. Two of the six propellers control the relative motion of the seesaw, and we showed that this configuration allows 5 DoFs (of the body) to be controlled independently. This concept is extended here to an octocopter with four seesaws. We demonstrate that all six body DoFs can be controlled independently, and that the yaw motion can be generated from the propellers' thrust rather than their pure torque, allowing for a more agile yaw motion. As explained, the current platform is an octocopter driven by eight propellers. Compared to a standard octocopter, the thrust tilting mechanism based on seesaws requires no additional weight.

II. Structure, Kinematics, and Dynamics

A. Structure

The structure of the drone is illustrated in Fig. 1. It includes eight propellers attached to the end of four seesaws. Two independent seesaws are positioned along the body x axis, while the other two are placed along the y. The seesaws are equally distanced from the center of mass such that the moments due to their weight is null. Each seesaw can rotate freely with respect to the body, and it is actuated by two propellers at its both ends. The difference between the thrust forces of the two propellers determines the angular motion of the seesaw relative to the body, while the total force of the two propellers affects the motion of the drone. The described

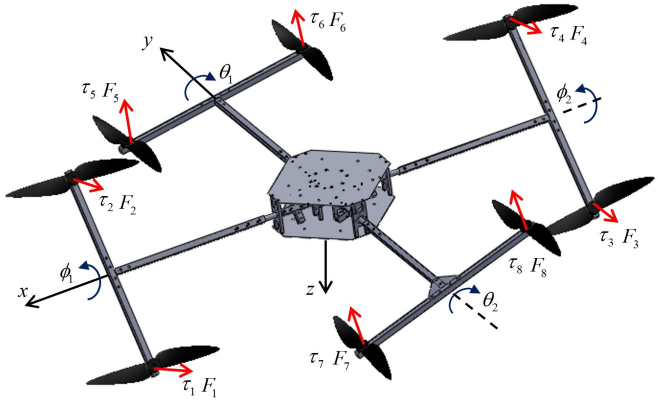

Fig. 1. The structure of the four-seesaw octocopter

[1]Dolev Yecheskel completed his Master's degree at the department of mechanical engineering, Ben-Gurion University of the Negev, Israel.

[2]Shai Arogeti is with the department of mechanical engineering, Ben-Gurion University of the Negev, Israel, (e-mail: arogeti@bgu.ac.il).

UAV has ten degrees of freedom, which are:

- The drone's position in space, given by (x,y,z), measured at the center of mass (3 DoFs).
- The body's angular state represented by the three Euler angles (ϕ,θ,ψ), roll, pitch and yaw (3 DoFs).
- The angular state of the four seesaws with respect to the body; these are independent variables (4 DoFs).

The motion of the drone is affected by the state of the four seesaws, and generally, all of its ten DoFs are coupled. To achieve a certain motion of the drone's body, a certain seesaws' configuration is needed. Nevertheless, we will show that this configuration is not unique, allowing us some freedom in the control design.

B. Kinematics

The kinematic relations are derived from the relation between the two main systems of coordinate, the NED inertial system, notated by $\hat{e}=\begin{bmatrix}\hat{x}_e & \hat{y}_e & \hat{z}_e\end{bmatrix}^T$ (with z pointing down), and the body coordinate system $\hat{b}=\begin{bmatrix}\hat{x}_b & \hat{y}_b & \hat{z}_b\end{bmatrix}^T$, attached to the center of gravity. Assume that R_x is the rotation matrix that describes roll (ϕ), R_y describes pitch (θ), and R_z yaw (ψ), the rotation matrix between the two mentioned coordinate systems (with $C\doteq\cos$ and $S\doteq\sin$) is given by,

$$\begin{aligned}R &= R_z R_y R_x \\ &= \begin{bmatrix} C_\theta C_\psi & S_\phi S_\theta C_\psi - C_\phi S_\psi & C_\phi S_\theta C_\psi + S_\phi S_\psi \\ C_\theta S_\psi & S_\phi S_\theta S_\psi + C_\phi C_\psi & S_\phi S_\theta C_\psi - S_\phi C_\psi \\ -S_\theta & S_\phi C_\theta & C_\phi C_\theta \end{bmatrix}. \end{aligned} \quad (1)$$

To express the relation between the drone's angular velocity in the inertial frame (represented by $\omega=\begin{bmatrix}\omega_x & \omega_y & \omega_z\end{bmatrix}^T$) and the time derivative of Euler angles, we use the relation $\mathbf{S}(\omega)=\dot{R}R^T$ (with $\mathbf{S}(\cdot)$ skew-symmetric). This yields,

$$\begin{bmatrix}\omega_x\\ \omega_y\\ \omega_z\end{bmatrix} = \begin{bmatrix} C_\theta C_\psi & -S_\psi & 0 \\ C_\theta S_\psi & C_\psi & 0 \\ -S_\theta & 0 & 1 \end{bmatrix} \begin{bmatrix}\dot{\phi}\\ \dot{\theta}\\ \dot{\psi}\end{bmatrix} = J_\omega \begin{bmatrix}\dot{\phi}\\ \dot{\theta}\\ \dot{\psi}\end{bmatrix} \quad (2)$$

where the matrix J_ω is the rotational Jacobian ([10]). The angular velocity with respect to the body frame is then,

$$\Omega = \begin{bmatrix}p\\ q\\ r\end{bmatrix} = R^T \begin{bmatrix}\omega_x\\ \omega_y\\ \omega_y\end{bmatrix} = R^T J_\omega \begin{bmatrix}\dot{\phi}\\ \dot{\theta}\\ \dot{\psi}\end{bmatrix} = J_{\Omega b} \begin{bmatrix}\dot{\phi}\\ \dot{\theta}\\ \dot{\psi}\end{bmatrix} \quad (3)$$

with,

$$J_{\Omega b} = \begin{bmatrix} 1 & 0 & -S_\theta \\ 0 & C_\phi & S_\phi C_\theta \\ 0 & -S_\phi & C_\phi C_\theta \end{bmatrix}.$$

Four additional local coordinate systems are defined to describe the motion of seesaws. They are attached to the seesaw frames. Each seesaw has a single DoF relative to the body; hence four angles are defined: ϕ_1 and ϕ_2 to describe the relative motion of the two seesaws on the x axis (see Fig. 1) and θ_1,θ_2 that describe the two seesaws on y. The following four rotation matrices represent the relative motion of the seesaws with respect to the body,

$$\begin{aligned} {}^{\hat{b}}R_{\phi_1} &= \begin{bmatrix} 1 & 0 & 0 \\ 0 & C_{\phi_1} & -S_{\phi_1} \\ 0 & S_{\phi_1} & C_{\phi_1} \end{bmatrix}, \; {}^{\hat{b}}R_{\phi_2} = \begin{bmatrix} 1 & 0 & 0 \\ 0 & C_{\phi_2} & -S_{\phi_2} \\ 0 & S_{\phi_2} & C_{\phi_2} \end{bmatrix} \\ {}^{\hat{b}}R_{\theta_1} &= \begin{bmatrix} C_{\theta_1} & 0 & S_{\theta_1} \\ 0 & 1 & 0 \\ -S_{\theta_1} & 0 & C_{\theta_1} \end{bmatrix}, \; {}^{\hat{b}}R_{\theta_2} = \begin{bmatrix} C_{\theta_2} & 0 & S_{\theta_2} \\ 0 & 1 & 0 \\ -S_{\theta_2} & 0 & C_{\theta_2} \end{bmatrix}. \end{aligned} \quad (4)$$

The total thrust generated by each couple of propellers (in a single seesaw) works in the z direction of the local coordinate system. Earlier, we mentioned the relation between the time derivative of Euler angles and the angular velocity vector of the body. In a similar way, we develop an expression for the angular velocity of a seesaw with respect to the inertial frame as a function of its relative motion and time derivative of Euler angles. We will only develop the Jacobian related to θ_1 here, while the rest can be developed similarly. For that, we use $\mathbf{S}(\omega_{\theta_1})={}^e\dot{R}_{\theta_1}({}^eR_{\theta_1})^T$, with ${}^eR_{\theta_1}=R({}^{\hat{b}}R_{\theta_1})$, to yield,

$$\omega_{e\theta_1} = \begin{bmatrix}\omega_{x\theta_1}\\ \omega_{y\theta_1}\\ \omega_{z\theta_1}\end{bmatrix} = J_{\omega\theta_1} \begin{bmatrix}\dot{\phi}\\ \dot{\theta}\\ \dot{\psi}\\ \dot{\theta}_1\end{bmatrix} \quad (5)$$

which, with respect to the body frame, becomes,

$$J_{\Omega\theta_1} = R^T J_{\omega\theta_1} = \begin{bmatrix} C_{\theta_1} & S_\phi S_{\theta_1} & -C_{\theta_1}S_\theta - C_\phi C_\theta S_{\theta_1} & 0 \\ 0 & C_\phi & S_\phi C_\theta & 1 \\ S_{\theta_1} & -S_\phi C_{\theta_1} & C_\phi C_\theta C_{\theta_1} - S_\theta S_{\theta_1} & 0 \end{bmatrix}.$$

For the formulation of the dynamical model in the next section, we extend the Jacobian in the following way,

$$\Omega_{\theta_1} = \begin{bmatrix}p_{\theta_1}\\ q_{\theta_1}\\ r_{\theta_1}\end{bmatrix} = \bar{J}_{\Omega\theta_1}\dot{\sigma}, \quad (6)$$

$$\sigma = \begin{bmatrix}\phi & \theta & \psi & \phi_1 & \phi_2 & \theta_1 & \theta_2\end{bmatrix}^T \quad (7)$$

where,

$$\bar{J}_{\Omega\theta_1} = \begin{bmatrix} C_{\theta_1} & S_\phi S_{\theta_1} & -C_{\theta_1}S_\theta - C_\phi C_\theta S_{\theta_1} & 0 & 0 & 0 & 0 \\ 0 & C_\phi & S_\phi C_\theta & 0 & 0 & 1 & 0 \\ S_{\theta_1} & -S_\phi C_{\theta_1} & C_\phi C_\theta C_{\theta_1} - S_\theta S_{\theta_1} & 0 & 0 & 0 & 0 \end{bmatrix}.$$

The vector σ combines all of the angular states of the drone, including the four seesaws. It will be used in the development the equations of motion, and the design of the angular states controller. As mentioned, $\bar{J}_{\Omega\theta_2}$, $\bar{J}_{\Omega\phi_1}$ and $\bar{J}_{\Omega\phi_2}$ are developed in a similar way to $\bar{J}_{\Omega\theta_1}$, and $\bar{J}_{\Omega b}$ is the extension of $J_{\Omega b}$.

C. Dynamics

Assume the standard static relation between the thrust and torque generated by a propeller and its angular speed, i.e.,

$$F_i = \gamma_1\omega_i^2 \quad , \qquad \tau_i = \gamma_2\omega_i^2 \quad (8)$$

where, F_i thrust, τ_i torque, ω_i angular speed and γ_1,γ_2 are constants. The index i represents the propeller number according to Fig. 1. The platform has eight propellers responsible for the net motion of the drone's body and the relative

state of the seesaws. Concerning the drone's structure in Fig. 1, we emphasize the following:

- Propellers 1 and 2 belong to the seesaw on the positive side of the body axis x. A larger thrust by propeller 1 causes an angular motion in the positive direction of ϕ_1.
- Propellers 3 and 4 belong to the seesaw on the negative side of x. A larger thrust by propeller 3 causes an angular motion in the positive direction of ϕ_2.
- Propellers 5 and 6 are on the positive side of y. A larger thrust by propeller 5 causes angular motion in the positive direction of θ_1.
- Propellers 7 and 8 are on the negative side of y. A larger thrust by propeller 7 causes an angular motion in the positive direction of θ_2.

We are particularly interested in the controlled motion of the body; hence we now express the forces acting in the direction of $\hat{x}_b,\hat{y}_b,\hat{z}_b$ (the body coordinates). These forces depend on the relative state of the seesaws and the body. Hence, using the rotation matrices in (4), we can write,

$$F_{1,2}^{\hat{b}} = {}^{\hat{b}}R_{\phi_1}\begin{bmatrix}0\\0\\-F_{1,2}\end{bmatrix} = -(F_1+F_2)\begin{bmatrix}0\\-\sin\phi_1\\\cos\phi_1\end{bmatrix} \tag{9}$$

where $F_{1,2} = (F_1+F_2)$ is the total thrust generated by propellers 1 and 2 in the local z direction. Continuing with this line, we can formulate the body forces as,

$$\begin{aligned}
F_{tx}^{\hat{b}} &= -(F_5+F_6)\sin\theta_1 - (F_7+F_8)\sin\theta_2\\
F_{ty}^{\hat{b}} &= (F_1+F_2)\sin\phi_1 + (F_3+F_4)\sin\phi_2\\
F_{tz}^{\hat{b}} &= -(F_1+F_2)\cos\phi_1 - (F_3+F_4)\cos\phi_2\\
&\quad -(F_5+F_6)\cos\theta_1 - (F_7+F_8)\cos\theta_2.
\end{aligned} \tag{10}$$

To formulate the moments acting on the drone's body and seesaws, two distances, d and l, are defined. They represent respectively the distance from a propeller to the center of the seesaw and the distance between the center of the seesaw and the center of gravity of the drone. Using these definitions, the four moments acting on the seesaws are,

$$\begin{aligned}
\tau_{\phi_1} &= d(F_1-F_2) \quad , \quad \tau_{\phi_2} = d(F_3-F_4)\\
\tau_{\theta_1} &= d(F_5-F_6) \quad , \quad \tau_{\theta_2} = d(F_7-F_8)
\end{aligned} \tag{11}$$

and the moments acting on the drone's body,

$$\begin{aligned}
\tau_\phi &= l(F_5+F_6)\cos\theta_1 - l(F_7+F_8)\cos\theta_2\\
&\quad +(\tau_5-\tau_6)\sin\theta_1 + (\tau_7-\tau_8)\sin\theta_2\\
\tau_\theta &= l(F_1+F_2)\cos\phi_1 - l(F_3+F_4)\cos\phi_2\\
&\quad +(\tau_1-\tau_2)\sin\phi_1 + (\tau_3-\tau_4)\sin\phi_2\\
\tau_\psi &= l(F_1+F_2)\sin\phi_1 - l(F_3+F_4)\sin\phi_2\\
&\quad +(-\tau_1+\tau_2)\cos\phi_1 + (\tau_3-\tau_4)\cos\phi_2\\
&\quad +l(F_5+F_6)\sin\theta_1 - l(F_7+F_8)\sin\theta_2\\
&\quad +(-\tau_5+\tau_6)\cos\theta_1 + (\tau_7-\tau_8)\cos\theta_2.
\end{aligned} \tag{12}$$

We are interested in a controller that allows independent control of all six DoFs of the drone's body, i.e., its position and orientation. To obtain the force and torque needed to stabilize the body, it is necessary to determine the equivalent thrust force and moment in each seesaw. The relevant relations amount to a system of six equations and eight unknowns. This redundancy provides us with some freedom in the choice of some of the unknowns. For the relevant equations, we use $F_{1,2}$ as the equivalent thrust in the seesaw of propellers 1 and 2, and a similar notation for all four seesaws. These four thrusts are the first four unknowns; the other four are the four equivalent moments generated in the seesaws due to different thrusts (on both sides). As a first step, we relate the thrust and torque of a single propeller in the following way,

$$\begin{matrix}\tau = \gamma_2\omega^2\\ F = \gamma_1\omega^2\end{matrix} \quad \Rightarrow \quad \frac{\tau}{F} = \frac{\gamma_2}{\gamma_1}. \tag{13}$$

If identical propellers are used, then, the ratio in (13) works also for a combination of thrusts and torques, that is,

$$\begin{matrix}(\tau_1-\tau_2) = \gamma_2(\omega_1^2-\omega_2^2)\\ (F_1-F_2) = \gamma_1(\omega_1^2-\omega_2^2)\end{matrix} \quad \Rightarrow \quad \frac{(\tau_1-\tau_2)}{(F_1-F_2)} = \frac{\gamma_2}{\gamma_1}. \tag{14}$$

Using (14), we can reformulate (11), as,

$$\begin{aligned}
\tau_{\phi_1} = d(\tau_1-\tau_2)\frac{\gamma_1}{\gamma_2} \quad &\Rightarrow \quad (\tau_1-\tau_2) = \tau_{\phi_1}\frac{\gamma_2}{\gamma_1 d}\\
\tau_{\phi_2} = d(\tau_3-\tau_4)\frac{\gamma_1}{\gamma_2} \quad &\Rightarrow \quad (\tau_3-\tau_4) = \tau_{\phi_2}\frac{\gamma_2}{\gamma_1 d}\\
\tau_{\theta_1} = d(\tau_5-\tau_6)\frac{\gamma_1}{\gamma_2} \quad &\Rightarrow \quad (\tau_5-\tau_6) = \tau_{\theta_1}\frac{\gamma_2}{\gamma_1 d}\\
\tau_{\theta_2} = d(\tau_7-\tau_8)\frac{\gamma_1}{\gamma_2} \quad &\Rightarrow \quad (\tau_7-\tau_8) = \tau_{\theta_2}\frac{\gamma_2}{\gamma_1 d}.
\end{aligned} \tag{15}$$

From (10), (12), and (15), a system of six equations is obtained that relates seesaws thrust and moments with body forces and torques,

$$\begin{aligned}
F_{tx}^{\hat{b}} &= -F_{5,6}\sin\theta_1 - F_{7,8}\sin\theta_2\\
F_{ty}^{\hat{b}} &= F_{1,2}\sin\phi_1 + F_{3,4}\sin\phi_2\\
F_{tz}^{\hat{b}} &= -F_{1,2}\cos\phi_1 - F_{3,4}\cos\phi_2 - F_{5,6}\cos\theta_1 - F_{7,8}\cos\theta_2
\end{aligned} \tag{16}$$

$$\begin{aligned}
\tau_\phi &= lF_{5,6}\cos\theta_1 - lF_{7,8}\cos\theta_2 + \tau_{\theta_1}\frac{\gamma_2}{d\gamma_1}\sin\theta_1 + \tau_{\theta_2}\frac{\gamma_2}{d\gamma_1}\sin\theta_2\\
\tau_\theta &= lF_{1,2}\cos\phi_1 - lF_{3,4}\cos\phi_2 + \tau_{\phi_1}\frac{\gamma_2}{d\gamma_1}\sin\phi_1 + \tau_{\phi_2}\frac{\gamma_2}{d\gamma_1}\sin\phi_2\\
\tau_\psi &= lF_{1,2}\sin\phi_1 - lF_{3,4}\sin\phi_2 - \tau_{\phi_1}\frac{\gamma_2}{d\gamma_1}\cos\phi_1 + \tau_{\phi_2}\frac{\gamma_2}{d\gamma_1}\cos\phi_2\\
&\quad + lF_{5,6}\sin\theta_1 - lF_{7,8}\sin\theta_2 + \tau_{\theta_1}\frac{\gamma_2}{d\gamma_1}\cos\theta_1 + \tau_{\theta_2}\frac{\gamma_2}{d\gamma_1}\cos\theta_2.
\end{aligned} \tag{17}$$

Obviously, the equivalent thrust and moment of a seesaw are not the actual control inputs; hence, they should be related to the propellers angular speeds. This is expressed by the following,

$$\begin{aligned}
\bar{u} &\doteq \begin{bmatrix}F_{1,2} & F_{3,4} & F_{5,6} & F_{7,8} & \tau_{\phi_1} & \tau_{\phi_2} & \tau_{\theta_1} & \tau_{\theta_2}\end{bmatrix}^T\\
\bar{\omega} &\doteq \begin{bmatrix}\omega_1^2 & \omega_2^2 & \omega_3^2 & \omega_4^2 & \omega_5^2 & \omega_6^2 & \omega_7^2 & \omega_8^2\end{bmatrix}^T\\
\bar{u} &= A_{\text{act}}\bar{\omega}
\end{aligned} \tag{18}$$

where,

$$A_{\text{act}} = \begin{bmatrix} \gamma_1 & \gamma_1 & 0 & 0 & 0 & 0 & 0 & 0 \\ 0 & 0 & \gamma_1 & \gamma_1 & 0 & 0 & 0 & 0 \\ 0 & 0 & 0 & 0 & \gamma_1 & \gamma_1 & 0 & 0 \\ 0 & 0 & 0 & 0 & 0 & 0 & \gamma_1 & \gamma_1 \\ d\gamma_1 & -d\gamma_1 & 0 & 0 & 0 & 0 & 0 & 0 \\ 0 & 0 & d\gamma_1 & -d\gamma_1 & 0 & 0 & 0 & 0 \\ 0 & 0 & 0 & 0 & d\gamma_1 & -d\gamma_1 & 0 & 0 \\ 0 & 0 & 0 & 0 & 0 & 0 & d\gamma_1 & -d\gamma_1 \end{bmatrix}.$$

Since this matrix is invertible, the actual control inputs can be calculated given a required set of seesaws' equivalent forces and moments (that are the control inputs for the following design).

III. Equations of Motion

Here, we develop the drone's equations of motion from the Euler-Lagrange approach. We assume that under the studied flight conditions, drag and friction forces are negligible. The generalized coordinates include the position and orientation of the drone's body, together with the four relative angels of the seesaws; hence we have,

$$\bar{q} = \begin{bmatrix} x & y & z & \phi & \theta & \psi & \phi_1 & \phi_2 & \theta_1 & \theta_2 \end{bmatrix}^T. \quad (19)$$

Denoting the position coordinates by $\xi = \begin{bmatrix} x & y & z \end{bmatrix}^T$, the kinetic energy, which consists of the energy of five bodies, is,

$$\begin{aligned} T = &\frac{1}{2} m \dot{\xi}^T \dot{\xi} + \frac{1}{2} \omega_e{}^T I_e \omega_e \\ &+ \frac{1}{2} \omega_{e\phi_1}^T I_{e\phi_1} \omega_{e\phi_1} + \frac{1}{2} \omega_{e\phi_2}^T I_{e\phi_2} \omega_{e\phi_2} \\ &+ \frac{1}{2} \omega_{e\theta_1}^T I_{e\theta_1} \omega_{e\theta_1} + \frac{1}{2} \omega_{e\theta_2}^T I_{e\theta_2} \omega_{e\theta_2} \end{aligned} \quad (20)$$

where, ω_e is the angular velocity of the body, $\omega_{e\phi_1}$, $\omega_{e\phi_2}$, $\omega_{e\theta_1}$ and $\omega_{e\theta_2}$ are the angular velocities of the seesaws, and I_e, $I_{e\phi_1}$, $I_{e\phi_2}$, $I_{e\theta_1}$, and $I_{e\theta_2}$ are rotational inertia matrices; all are given with respect to the inertial frame. For the Lagrangian, we express the potential energy by,

$$U = -mg\xi^T e_3 \quad (21)$$

where, $e_3 = \begin{bmatrix} 0 & 0 & 1 \end{bmatrix}^T$ is a basis vector. The rotational inertia matrices are transformed from the local coordinates to the inertial coordinates using the following relations,

$$\begin{aligned} &I_e = R I_b R^T \\ &I_{e\phi_1} = R^{\hat{b}} R_{\phi_1} I_{b\phi_1}{}^{\hat{b}} R_{\phi_1}^T R^T, \quad I_{e\phi_2} = R^{\hat{b}} R_{\phi_2} I_{b\phi_2}{}^{\hat{b}} R_{\phi_2}^T R^T \\ &I_{e\theta_1} = R^{\hat{b}} R_{\theta_1} I_{b\theta_1}{}^{\hat{b}} R_{\theta_1}^T R^T, \quad I_{e\theta_2} = R^{\hat{b}} R_{\theta_2} I_{b\theta_2}{}^{\hat{b}} R_{\theta_2}^T R^T. \end{aligned} \quad (22)$$

Adding the assumption that all bodies are symmetric, the four seesaws' rotational inertia matrices with respect to the local coordinates (i.e., $I_{b\phi_1}$, $I_{b\phi_2}$, $I_{b\theta_1}$ and $I_{b\theta_2}$) are diagonal. As to the rotational inertia matrix of the body, we assume that two opposite seesaws (i.e., seesaws of the same body axis) move in almost identical angles such that the matrix can be assumed symmetric. The kinetic energy in (20) is naturally formulated with angular velocity vectors. Since Euler angles, $\eta \doteq \begin{bmatrix} \phi & \theta & \psi \end{bmatrix}^T$, represent the angular state, it would be more consistent if the kinetic energy is also formulated by the time derivatives of Euler angles. For that, the rotational Jacobian matrices (2) and (5) are applied to yield,

$$\begin{aligned} T = &\frac{1}{2} m \dot{\xi}^T \dot{\xi} + \frac{1}{2} \dot{\eta}^T J_\omega^T R I_b R^T J_\omega \dot{\eta} \\ &+ \frac{1}{2} \begin{bmatrix} \dot{\eta} \\ \dot{\phi}_1 \end{bmatrix}^T J_{\omega\phi_1}^T R^{\hat{b}} R_{\phi_1} I_{b\phi_1}{}^{\hat{b}} R_{\phi_1}^T R^T J_{\omega\phi_1} \begin{bmatrix} \dot{\eta} \\ \dot{\phi}_1 \end{bmatrix} \\ &+ \frac{1}{2} \begin{bmatrix} \dot{\eta} \\ \dot{\phi}_2 \end{bmatrix}^T J_{\omega\phi_2}^T R^{\hat{b}} R_{\phi_2} I_{b\phi_2}{}^{\hat{b}} R_{\phi_2}^T R^T J_{\omega\phi_2} \begin{bmatrix} \dot{\eta} \\ \dot{\phi}_2 \end{bmatrix} \\ &+ \frac{1}{2} \begin{bmatrix} \dot{\eta} \\ \dot{\theta}_1 \end{bmatrix}^T J_{\omega\theta_1}^T R^{\hat{b}} R_{\theta_1} I_{b\theta_1}{}^{\hat{b}} R_{\theta_1}^T R^T J_{\omega\theta_1} \begin{bmatrix} \dot{\eta} \\ \dot{\theta}_1 \end{bmatrix} \\ &+ \frac{1}{2} \begin{bmatrix} \dot{\eta} \\ \dot{\theta}_2 \end{bmatrix}^T J_{\omega\theta_2}^T R^{\hat{b}} R_{\theta_2} I_{b\theta_2}{}^{\hat{b}} R_{\theta_2}^T R^T J_{\omega\theta_2} \begin{bmatrix} \dot{\eta} \\ \dot{\theta}_2 \end{bmatrix}. \end{aligned} \quad (23)$$

As the kinetic energy does not depend on the choice of a coordinate system, an alternative formulation of (23) is such that the energy is expressed in the local coordinates. This is done by replacing the representation of the Jacobian matrices, e.g., $J_\Omega = R^T J_\omega$. The obtained kinetic energy (that is parallel to (23)) is,

$$\begin{aligned} T = &\frac{1}{2} m \dot{\xi}^T \dot{\xi} + \frac{1}{2} \dot{\eta}^T J_{\Omega b}^T I_b J_{\Omega b} \dot{\eta} \\ &+ \frac{1}{2} \begin{bmatrix} \dot{\eta} \\ \dot{\phi}_1 \end{bmatrix}^T J_{\Omega\phi_1}^T I_{b\phi_1} J_{\Omega\phi_1} \begin{bmatrix} \dot{\eta} \\ \dot{\phi}_1 \end{bmatrix} + \frac{1}{2} \begin{bmatrix} \dot{\eta} \\ \dot{\phi}_2 \end{bmatrix}^T J_{\Omega\phi_2}^T I_{b\phi_2} J_{\Omega\phi_2} \begin{bmatrix} \dot{\eta} \\ \dot{\phi}_2 \end{bmatrix} \\ &+ \frac{1}{2} \begin{bmatrix} \dot{\eta} \\ \dot{\theta}_1 \end{bmatrix}^T J_{\Omega\theta_1}^T I_{b\theta_1} J_{\Omega\theta_1} \begin{bmatrix} \dot{\eta} \\ \dot{\theta}_1 \end{bmatrix} + \frac{1}{2} \begin{bmatrix} \dot{\eta} \\ \dot{\theta}_2 \end{bmatrix}^T J_{\Omega\theta_2}^T I_{b\theta_2} J_{\Omega\theta_2} \begin{bmatrix} \dot{\eta} \\ \dot{\theta}_2 \end{bmatrix}. \end{aligned} \quad (24)$$

Using the definition of σ from (7) and the extended Jacobian formulation (6), the final formulation of T for our needs is,

$$\begin{aligned} T = &\frac{1}{2} m \dot{\xi}^T \dot{\xi} + \frac{1}{2} \dot{\sigma}^T \bar{J}_{\Omega b}^T I_b \bar{J}_{\Omega b} \dot{\sigma} \\ &+ \frac{1}{2} \dot{\sigma}^T \bar{J}_{\Omega\phi_1}^T I_{b\phi_1} \bar{J}_{\Omega\phi_1} \dot{\sigma} + \frac{1}{2} \dot{\sigma}^T \bar{J}_{\Omega\phi_2}^T I_{b\phi_2} \bar{J}_{\Omega\phi_2} \dot{\sigma} \\ &+ \frac{1}{2} \dot{\sigma}^T \bar{J}_{\Omega\theta_1}^T I_{b\theta_1} \bar{J}_{\Omega\theta_1} \dot{\sigma} + \frac{1}{2} \dot{\sigma}^T \bar{J}_{\Omega\theta_2}^T I_{b\theta_2} \bar{J}_{\Omega\theta_2} \dot{\sigma}. \end{aligned} \quad (25)$$

To simplify (25), a unified rotational inertia matrix, $D \in \mathbb{R}^{7\times 7}$, is defined by,

$$\begin{aligned} D = &\bar{J}_{\Omega b}^T I_b \bar{J}_{\Omega b} + \bar{J}_{\Omega\phi_1}^T I_{b\phi_1} \bar{J}_{\Omega\phi_1} + \bar{J}_{\Omega\phi_2}^T I_{b\phi_2} \bar{J}_{\Omega\phi_2} \\ &+ \bar{J}_{\Omega\theta_1}^T I_{b\theta_1} \bar{J}_{\Omega\theta_1} + \bar{J}_{\Omega\theta_2}^T I_{b\theta_2} \bar{J}_{\Omega\theta_2} \end{aligned} \quad (26)$$

which puts (25) in the following compact form,

$$T = \frac{1}{2} m \dot{\xi}^T \dot{\xi} + \frac{1}{2} \dot{\sigma}^T D \dot{\sigma}. \quad (27)$$

Recall (21), the obtained Lagrangian is therefore,

$$L = T - U = \frac{1}{2} m \dot{\xi}^T \dot{\xi} + \frac{1}{2} \dot{\sigma}^T D \dot{\sigma} + mg\xi^T e_3. \quad (28)$$

To develop the equations of motion, we apply the second form of the Euler-Lagrange equation, namely,

$$\frac{\partial}{\partial t} \left(\frac{\partial L}{\partial \dot{q}} \right) - \frac{\partial L}{\partial q} = \begin{bmatrix} F_\xi \\ \tau_\sigma \end{bmatrix} \quad (29)$$

where, $\tau_\sigma = \begin{bmatrix}\tau_\phi & \tau_\theta & \tau_\psi & \tau_{\phi_1} & \tau_{\phi_2} & \tau_{\theta_1} & \tau_{\theta_2}\end{bmatrix}^T$, as is defined in (15) and (17). The non-conservative forces, represented on the inertial frame, are obtained by transforming the forces in (16) (by R), which gives,

$$F_\xi = R \begin{bmatrix} F_{tx}^{\hat{b}} \\ F_{ty}^{\hat{b}} \\ F_{tz}^{\hat{b}} \end{bmatrix}. \tag{30}$$

To continue, we divide (29) into two equations, one for position coordinates (ξ) and another for angular coordinates (σ). The first equation is,

$$\frac{\partial}{\partial t}\left(\frac{\partial L}{\partial \dot{\xi}}\right) - \frac{\partial L}{\partial \xi} = F_\xi \tag{31}$$

which gives,

$$\frac{\partial L}{\partial \dot{\xi}} = m\dot{\xi}, \quad \frac{\partial}{\partial t}\left(\frac{\partial L}{\partial \dot{\xi}}\right) = m\ddot{\xi}, \quad \frac{\partial L}{\partial \xi} = mge_3$$

$$\Rightarrow \quad \ddot{\xi} = ge_3 + \frac{1}{m}F_\xi = \begin{bmatrix}\ddot{x}\\ \ddot{y}\\ \ddot{z}\end{bmatrix} = \begin{bmatrix}0\\0\\g\end{bmatrix} + \frac{1}{m}R\begin{bmatrix} F_{tx}^{\hat{b}} \\ F_{ty}^{\hat{b}} \\ F_{tz}^{\hat{b}} \end{bmatrix}. \tag{32}$$

These are the drone's translational motion equations. For the angular motion, we have,

$$\frac{dL}{d\dot{\sigma}} = D(\sigma)\dot{\sigma}, \quad \frac{d}{dt}\left(\frac{dL}{d\dot{\sigma}}\right) = D(\sigma)\ddot{\sigma} + \dot{D}(\sigma)\dot{\sigma}$$
$$\frac{dL}{d\sigma} = \frac{1}{2}\frac{d}{d\sigma}\left[\dot{\sigma}^T D(\sigma)\dot{\sigma}\right]$$

which amounts to,

$$D(\sigma)\ddot{\sigma} = \left\{\tau_\sigma + \frac{1}{2}\frac{d}{d\sigma}\left[\dot{\sigma}^T D(\sigma)\dot{\sigma}\right] - \dot{D}(\sigma)\dot{\sigma}\right\}.$$

This compact relation describes all seven angular states. It can be further simplified to,

$$\ddot{\sigma} = D^{-1}(\sigma)\left[\tau_\sigma + C(\sigma,\dot{\sigma})\dot{\sigma}\right] \tag{33}$$

by defining $C(\sigma,\dot{\sigma}) = \frac{1}{2}\frac{d}{d\sigma}\left[\dot{\sigma}^T D(\sigma)\right] - \dot{D}(\sigma)$.

IV. Control System Design

A. Fully-actuated drone

We define a fully-actuated drone as a drone that all of its body six DoFs can be controlled independently. For that, we can show that the matrix multiplying the vector of inputs has a degree no less than the number DoFs to be controlled; it is not shown here due to space limitation.

B. Control system

The control system consists of two main elements; a stabilizer and a navigator. The stabilizer is in charge of stabilizing all (seven) angular states, while the navigator is responsible for motion in space. We adopt a hieratical structure where some of the desired angular states are determined by the navigator. As the number of independent inputs is eight (which are the elements in $\bar{\omega}$) and the number of independently controlled outputs is six (which are the body DoFs), the design is redundant, and some decisions are required to be taken. Similarly to [9], the closed-loop controllers are designed by the Integral Backstepping (IB) approach ([10]).

We start with the stabilizer; it is responsible for the convergence of $\sigma = \begin{bmatrix}\phi & \theta & \psi & \phi_1 & \phi_2 & \theta_1 & \theta_2\end{bmatrix}$ to desired values, given by $\sigma_d(t)$. Let $e_\sigma = \sigma_d - \sigma$ be the angular states error. The time derivative of the error is $\dot{e}_\sigma = \dot{\sigma}_d - \dot{\sigma}$. For convergence of e_σ to zero, we wish $\dot{\sigma}$ to follow the signal $\dot{\sigma}_w = c_1 e_\sigma + \dot{\sigma}_d + k_\sigma \chi_\sigma$, where $\chi_\sigma = \int_0^t e_\sigma d\tau$ and c_1, k_σ are positive definite matrices. Obviously, for $\dot{\sigma} = \dot{\sigma}_w$, the tracking error e_σ converges to zero exponentially. However, $\dot{\sigma}_w$ is not an independent control input; hence we define the error variable $e_{\sigma'} = \dot{\sigma}_w - \dot{\sigma}$, and calculate its time derivative (with the hope of bringing the actual control input into the equation). The result is, $\dot{e}_{\sigma'} = c_1\dot{e}_\sigma + \ddot{\sigma}_d + k_\sigma e_\sigma - \ddot{\sigma}$. At the next step, we substitute $\dot{e}_\sigma = -c_1 e_\sigma - k_\sigma\chi_\sigma + e_{\sigma'}$ to obtain,

$$\dot{e}_{\sigma'} = c_1(-c_1 e_\sigma - k_\sigma\chi_\sigma + e_{\sigma'}) + \ddot{\sigma}_d + k_\sigma e_\sigma - \ddot{\sigma}. \tag{34}$$

We wish that $e_{\sigma'}$ converges to zero exponential, hence we demand $\dot{e}_{\sigma'} = -c_2 e_{\sigma'} - e_\sigma$, with c_2 positive definite. This demand, together with (34), is equivalent to,

$$\ddot{\sigma} = \ddot{\sigma}_d + (I_{7x7} + k_\sigma - c_1 c_2)e_\sigma + (c_1 + c_2)\dot{e}_\sigma + c_2 k_\sigma \chi_\sigma. \tag{35}$$

The angular acceleration in (35) has the structure of a PID control signal with feedforward (i.e., $\ddot{\sigma}_d$). Defining $k_{P\sigma} = I_{7x7} + k_\sigma + c_1 c_2$, $k_{D\sigma} = c_1 + c_2$ and $k_{I\sigma} = c_2 k_\sigma$, and substituting (35) in (33), one has,

$$D^{-1}(\sigma)\left[\tau_\sigma + C(\sigma,\dot{\sigma})\dot{\sigma}\right] = \ddot{\sigma}_d + k_{P\sigma}e_\sigma + k_{D\sigma}\dot{e}_\sigma + k_{I\sigma}\chi_\sigma$$
$$\Rightarrow$$
$$\tau_\sigma = D(\sigma)\left\{\ddot{\sigma}_d + k_{P\sigma}e_\sigma + k_{D\sigma}\dot{e}_\sigma + k_{I\sigma}\chi_\sigma\right\} - C(\sigma,\dot{\sigma})\dot{\sigma}. \tag{36}$$

The asymptotic stability of the origin (i.e., $e_\sigma = e_{\sigma'} = 0$) can be concluded from the following Lyapunov function and its time derivative,

$$V = \frac{1}{2}\left\{\left[\chi_\sigma{}^T k_\sigma \chi_\sigma\right] + \left[e_\sigma{}^T e_\sigma\right] + \left[e_{\sigma'}{}^T e_{\sigma'}\right]\right\}$$
$$\Rightarrow$$
$$\dot{V} = \left[-e_\sigma{}^T c_1 e_\sigma\right] + \left[-e_{\sigma'}{}^T c_2 e_{\sigma'}\right] \le 0. \tag{37}$$

The stabilizer controls seven angular state variables. We assume that the first three (i.e., body angular state) are the choice of the operator, while the rest (seesaws angles) serve the navigator.

The navigator is the controller responsible for the motion on the desired spatial trajectory. It does so by determining the seesaws equivalent thrusts and desired angels. Nevertheless, there are more parameters to play with than those we want to control. Hence, a strategy should be determined, as will be explained in the following.

We start by designing the needed body thrust from the same IB approach as utilized for the angular states controller. Defining the position error by $e_\xi = \xi_d - \xi$, its time derivative is $\dot{e}_\xi = \dot{\xi}_d - \dot{\xi}$. To dictate the desired transient response of $\dot{e}_\xi$, we demand $\dot{\xi}$ to follow $\dot{\xi}_w = c_{\xi 1}e_\xi + \dot{\xi}_d + k_\xi\chi_\xi$ (where χ_ξ is integral of e_ξ and $c_{\xi 1}, k_\xi$ are positive definite matrices).

Hence, we wish $e_{\xi'} = \dot{\xi}_w - \dot{\xi}$ to converge to zero. From the time derivative $\dot{e}_{\xi'} = \ddot{\xi}_w - \ddot{\xi} = c_{\xi 1}\dot{e}_\xi + \ddot{\xi}_d + k_\xi e_\xi - \ddot{\xi}$ and after some algebra, we get,

$$\dot{e}_{\xi'} = c_{\xi 1}\left(-c_{\xi 1}e_\xi - k_\xi \chi_\xi + e_{\xi'}\right) + \ddot{\xi}_d + k_\xi e_\xi - \ddot{\xi} \tag{38}$$

that is equivalent to the structure of (38). To allow convergence of the error, we demand $\dot{e}_{\xi'} = -c_{\xi 2}e_{\xi'} - e_\xi$ (with $c_{\xi 2}$ positive definite), which amounts to,

$$\begin{aligned} &\ddot{\xi} = \ddot{\xi}_d + k_{P\xi}e_\xi + k_{D\xi}\dot{e}_\xi + k_{I\xi}\chi_\xi \\ &k_{P\xi} = I_{3x3} + k_\xi + c_{\xi 1}c_{\xi 2},\ k_{D\xi} = c_{\xi 1} + c_{\xi 2},\ k_{I\xi} = c_{\xi 2}k_\xi. \end{aligned} \tag{39}$$

Substituting this in the equations of motion, the required body forces are,

$$\begin{aligned} \begin{bmatrix} F_{tx}^{\hat{b}} \\ F_{ty}^{\hat{b}} \\ F_{tz}^{\hat{b}} \end{bmatrix} &= R^T\left[m\left(\ddot{\xi}_d + k_{P\xi}e_\xi + k_{D\xi}\dot{e}_\xi + k_{I\xi}\chi_\xi - ge_3\right)\right] \\ &\doteq R^T e_{con} = R^T\begin{bmatrix} e_{con,1} & e_{con,2} & e_{con,3} \end{bmatrix}^T \end{aligned} \tag{40}$$

We will design the navigator controller on a coordinate system rotated by ψ. This approach allows a temporal assumption of $\psi = 0$. Combining (40) with (16) gives,

$$\begin{aligned} -F_{5,6}\sin\theta_1 - F_{7,8}\sin\theta_2 &= \cos\theta\cdot e_{con,1} - \sin\theta\cdot e_{con,3} \\ F_{1,2}\sin\phi_1 + F_{3,4}\sin\phi_2 &= \sin\phi\sin\theta\cdot e_{con,1} \\ &\quad + \cos\phi\cdot e_{con,2} + \cos\theta\sin\phi\cdot e_{con,3} \\ -F_{1,2}\cos\phi_1 - F_{3,4}\cos\phi_2 - F_{5,6}\cos\theta_1 - F_{7,8}\cos\theta_2 &= \cos\phi\sin\theta\cdot e_{con,1} - \sin\phi\cdot e_{con,2} \\ &\quad + \cos\phi\cos\theta\cdot e_{con,3} \end{aligned} \tag{41}$$

The three equations in (41) represent the navigation demands. Satisfying these, allows tracking the reference trajectory. Note that here, the angular states are assumed known-functions of time (from sensors information). The angular state of the drone's body is governed by the three moments in (17). The elements in (17) related to the propeller's pure torque are generally much smaller than those obtained by thrusts differences (because γ_2 is two magnitudes of order smaller than γ_1 [10]). The seesaws allow quicker yaw motion by generating moments from thrust differences. Hence, we only use thrusts and thrust-tilting to control the angular states. Still, there are infinite combinations of actuation to achieve a desired motion. Generally, in the six equations (41) (for the desired translation), and (17) (for the desired angular state), one should solve for eight unknowns (the four equivalent thrusts $F_{1,2}, F_{3,4}, F_{5,6}, F_{7,8}$ and the four desired seesaw angles $\theta_{1d}, \theta_{2d}, \phi_{1d}, \phi_{2d}$). Hence, we take the following approach by determining,

$$F_{1-4} = \sqrt{\left(F_{ty}^{\hat{b}}\right)^2 + \left(F_{tz}^{\hat{b}}/2\right)^2}, \tag{42}$$

$$F_{5-8} = \sqrt{\left(F_{tx}^{\hat{b}}\right)^2 + \left(F_{tz}^{\hat{b}}/2\right)^2}. \tag{43}$$

where F_{1-4} is the total thrust of the four propellers $1-4$ (on the seesaws of ϕ_1, ϕ_2), and F_{5-8} is the total thrust of the rest (i.e., seesaws of θ_1, θ_2). By this approach, F_{1-4} generates the desired motion in the body's y direction, F_{5-8} works in the x direction, and the control effort along z is shared equally between the two propeller groups. Additionally, we decide that two opposite seesaws will have identical angles unless yaw moments are needed, hence,

$$\phi_{1,2} = \arcsin\left(F_{ty}^{\hat{b}}/F_{1-4}\right), \tag{44}$$

$$\theta_{1,2} = \arcsin\left(F_{tx}^{\hat{b}}/F_{5-8}\right). \tag{45}$$

Thus far, we have decided on the total thrust of the two clusters, F_{1-4} and F_{5-8}, but did not consider the thrusts needed for angular motions. To continue, we remind that $F_{3,4} = F_{1-4} - F_{1,2}$ and $F_{7,8} = F_{5-8} - F_{5,6}$, and decide that each opposite pair of seesaws will generate half of the moment required for yaw. This is done by slight deviations in the seesaw angles, formulated as,

$$\begin{aligned} \phi_{1d} &= \phi_{1,2} + e_{\phi_1} \quad , \quad \phi_{2d} = \phi_{1,2} - e_{\phi_1} \\ \theta_{1d} &= \theta_{1,2} + e_{\theta_1} \quad , \quad \theta_{2d} = \theta_{1,2} - e_{\theta_1}. \end{aligned} \tag{46}$$

Using these in the equations of the moments gives,

$$\begin{aligned} &\frac{F_{1,2}}{\cos e_{\phi_1}}\cos(\phi_{1,2} + e_{\phi_1}) - \frac{F_{1-4} - F_{1,2}}{\cos e_{\phi_1}}\cos(\phi_{1,2} - e_{\phi_1}) = \frac{\tau_\theta}{l} \\ &\frac{F_{1,2}}{\cos e_{\phi_1}}\sin(\phi_{1,2} + e_{\phi_1}) - \frac{F_{1-4} - F_{1,2}}{\cos e_{\phi_1}}\sin(\phi_{1,2} - e_{\phi_1}) = \frac{\tau_\psi}{2l} \\ &\frac{F_{5,6}}{\cos e_{\theta_1}}\cos(\theta_{1,2} + e_{\theta_1}) - \frac{F_{5-8} - F_{5,6}}{\cos e_{\theta_1}}\cos(\theta_{1,2} - e_{\theta_1}) = \frac{\tau_\phi}{l} \\ &\frac{F_{5,6}}{\cos e_{\theta_1}}\sin(\theta_{1,2} + e_{\theta_1}) - \frac{F_{5-8} - F_{5,6}}{\cos e_{\theta_1}}\sin(\theta_{1,2} - e_{\theta_1}) = \frac{\tau_\psi}{2l}. \end{aligned} \tag{47}$$

The last result includes four equations, from which, $F_{1,2}, F_{5,6}$, e_{ϕ_1} and e_{θ_1} are to be solved. The obtained solutions are,

$$\begin{aligned} e_{\phi_1} &= \arctan\left(\frac{\frac{\tau_\theta}{l\cos\phi_{1,2}} - \frac{\tau_\psi}{2l\sin\phi_{1,2}}}{-F_{1-4}\left(\tan\phi_{1,2} + \frac{1}{\tan\phi_{1,2}}\right)}\right) \\ F_{1,2} &= \frac{\tau_\theta}{2l\cos\phi_{1,2}} + \frac{F_{1-4}}{2}\left(1 + \tan\phi_{1,2}\tan e_{\phi_1}\right), \end{aligned} \tag{48}$$

$$\begin{aligned} e_{\theta_1} &= \arctan\left(\frac{\frac{\tau_\phi}{l\cos\theta_{1,2}} - \frac{\tau_\psi}{2l\sin\theta_{1,2}}}{-F_{5-8}\left(\tan\theta_{1,2} + \frac{1}{\tan\theta_{1,2}}\right)}\right) \\ F_{5,6} &= \frac{\tau_\phi}{2l\cos\theta_{1,2}} + \frac{F_{5-8}}{2}\left(1 + \tan\theta_{1,2}\tan e_{\theta_1}\right). \end{aligned} \tag{49}$$

Eventually, the two individual thrusts of each seesaw (that allow also the seesaws' local moments, τ_{ϕ_1}, τ_{ϕ_2}, τ_{θ_1} and τ_{θ_2}) can be calculated. For example, for the seesaw of F_1 and F_2,

$$\begin{matrix} F_1 + F_2 = F_{12} \\ d(F_1 - F_2) = \tau_{\phi_1} \end{matrix} \Rightarrow F_1 = \frac{F_{1,2} + \tau_{\phi_1}/d}{2}, \tag{50}$$

and identically for the rest of the seesaws.

C. Numerical results

We present two case studies that reflect the unique flying ability of the suggested drone. The moments of inertia in these examples are $I_x = I_y = 0.15\ [\mathrm{kg}\cdot\mathrm{m}^2]$ and $I_z = 0.3\ [\mathrm{kg}\cdot\mathrm{m}^2]$ for the drone's frame, and $I_{x\phi_1} = I_{x\phi_2} = I_{x\theta_1} = I_{x\theta_2} = 0.01\ [kg\cdot m^2]$, $I_{y\phi_1} = I_{y\phi_2} = I_{y\theta_1} = I_{y\theta_2} = 0.01\ [\mathrm{kg}\cdot\mathrm{m}^2]$, and $I_{z\phi_1} = I_{z\phi_2} = I_{z\theta_1} = I_{z\theta_2} = 0.02\ [\mathrm{kg}\cdot\mathrm{m}^2]$ for the seesaws. The drone's mass is $m = 1[\mathrm{kg}]$ with $l = 0.5[m]$ the distance of a seesaw from the center of gravity, and $d = 0.2[\mathrm{m}]$ as the distance of a propeller to the center of seesaw. We first examine the angular state controller only, while the controller gains are, $c_1 = 35 I_{7\times7}$, $c_2 = 10 I_{7\times7}$ and $k_\sigma = I_{7\times7}$. The result is shown in Fig. 2, with zero initial conditions, and with reference angles determined as (all angles in [rad]),

$$\phi_d = 0.1\sin(t), \quad \theta_d = 0.2\sin(t/2), \quad \psi_d = 2$$
$$\phi_{1d} = 0.3\cos(t), \quad \phi_{2d} = 0.1\sin(2t), \quad \theta_{1d} = t, \quad \theta_{2d} = 0.5t$$

In the following, the complete control system is working with the control gains,

$$c_1 = \begin{bmatrix} 19 I_{3\times3} & 0 \\ 0 & 35 I_{4\times4} \end{bmatrix}, \quad c_2 = \begin{bmatrix} 0.1 I_{3\times3} & 0 \\ 0 & 10 I_{4\times4} \end{bmatrix}$$
$$k_\sigma = \begin{bmatrix} 0.1 I_{3\times3} & 0 \\ 0 & I_{4\times4} \end{bmatrix}, \quad k_\xi = \begin{bmatrix} 0 & 0 & 0 \\ 0 & 0 & 0 \\ 0 & 0 & 2 \end{bmatrix}$$
$$c_{\xi_1} = 21 I_{3\times3}\ , \quad c_{\xi_2} = 0.3 I_{3\times3}.$$

The first case study (i.e., case study 1) shows convergence to a desired trajectory (of all body DoFs) defined by,

$$\phi_d = 1.2\sin(t)\ [\mathrm{rad}], \quad \theta_\mathrm{d} = 0.2\ [\mathrm{rad}], \quad \psi_\mathrm{d} = \pi/2\ [\mathrm{rad}]$$
$$x_d = 10\ [\mathrm{m}], \quad \mathrm{y_d} = \sin(\mathrm{t}/2)\ [\mathrm{m}], \quad \mathrm{z_d} = -\mathrm{t}/10\ [\mathrm{m}].$$

All initial conditions are zero, and the result is presented in Fig. 3 for the position coordinates and in Fig. 4 for the body angular states. Such six DoF trajectory tracking is not possible for standard drones. To get an impression of the work done by the seesaws, their angular motion is depicted in Fig. 5. We can see that opposite seesaws (of the same axis) move almost in parallel, which is consistent with the control strategy. The corresponding eight propellers' thrust forces are presented in Fig. 6.

The next case study (i.e., case study 2) demonstrates flight in extreme conditions. Here we demand that the body roll angle is $\pi/2$ for the first 15 [s] and then the desired roll is changed to π (i.e., the drone is upside-down). The reference state is then,

$$\phi_d = \pi/2\,(u(t) + u(t-15))\ [\mathrm{rad}], \quad \theta_\mathrm{d} = \psi_\mathrm{d} = 0\ [\mathrm{rad}]$$
$$x_d = t[\mathrm{m}], \quad \mathrm{y_d} = \sin(\mathrm{t}/2)\ [\mathrm{m}], \quad \mathrm{z_d} = -\mathrm{t}/10\ [\mathrm{m}]$$

with $u(t)$ as a step function, and the initial conditions are zero. The simulation result is shown in Fig. 7 (for the position) and in Fig. 8 for the roll angle. This result demonstrates the ability of the drone to fly on its side and on its back (such that the seesaws are completely flipped). To design the control system, the domain of the arcsin trigonometric function has been extended from $\left[-\pi/2 \quad \pi/2\right]$ to $\left[-\infty \quad \infty\right]$.

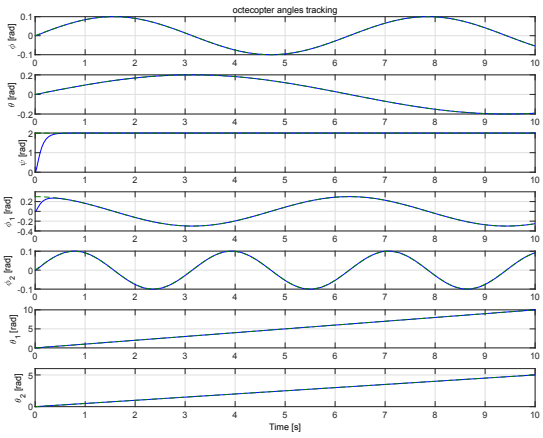

Fig. 2. Performance of the angular state controller.

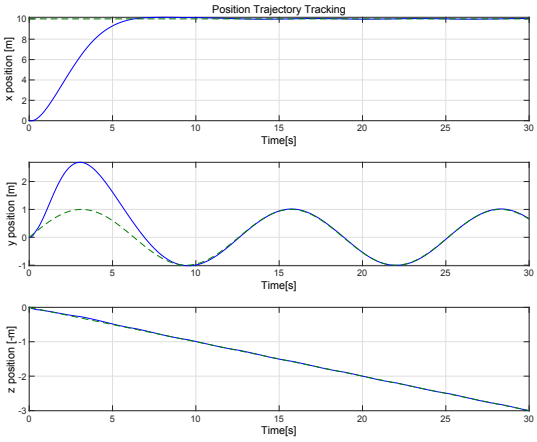

Fig. 3. Case study 1 - Drone's position coordinates.

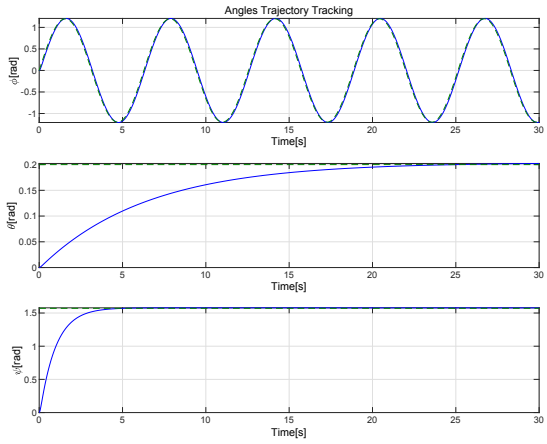

Fig. 4. Case study 1 - Drone's body angular coordinates.

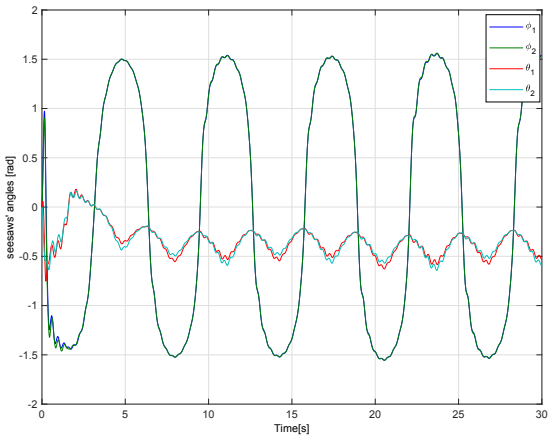

Fig. 5. Case study 1 - Angular states of seesaws.

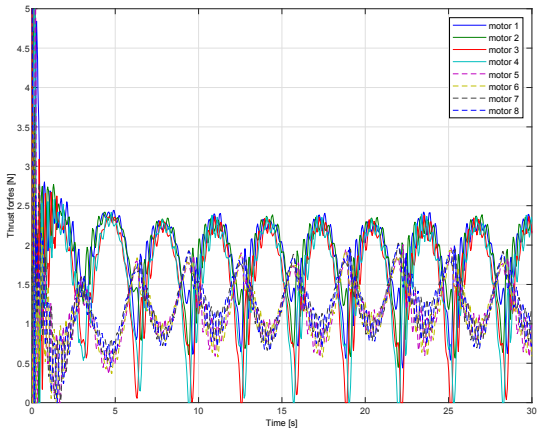

Fig. 6. Case study 1 - Propellers' thrust forces.

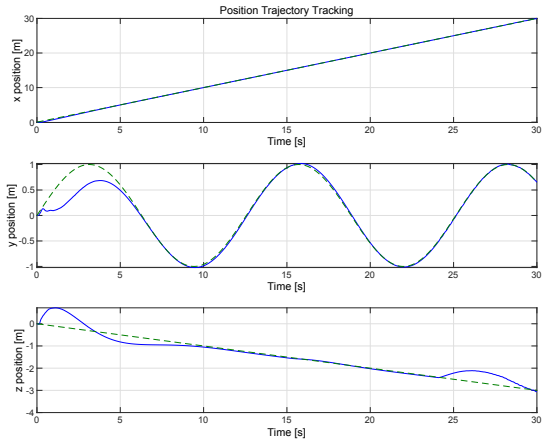

Fig. 7. Case study 2 - Drone's position coordinates.

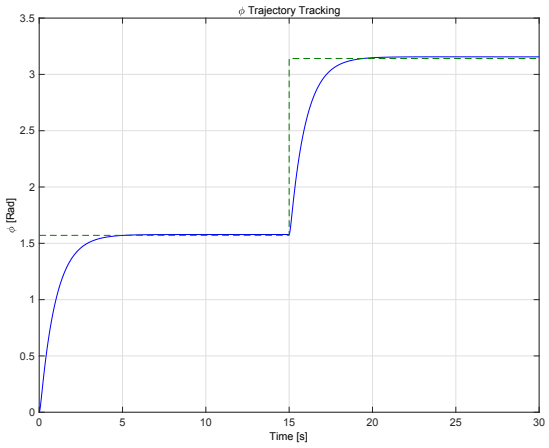

Fig. 8. Case study 2 - Drone's roll angle.

V. Conclusion

This paper suggested a fully actuated drone with a unique structure. The structure includes four freely rotating seesaws that allow tilting thrust forces. Unlike other drones with active tilting mechanisms (by additional servo motors), this drone is not required to carry additional actuators that do not directly contribute to the lift. Simulations have shown the performance of extreme maneuvers that are impossible with standard drones. Future work will include building a prototype where the four seesaw angles are measured by quadrature encoders and the body's angular state by a standard IMU.

References

[1] R. Rashad, J. Goerres, R. Aarts, J. B.C. Engelen, and S. Stramigioli, "Fully Actuated Multirotor UAVs: A Literature Review," IEEE Robotics Automation Magazine, Vol. 27, Issue 3, 2020.

[2] D. Langkamp, G. Roberts, A. Scillitoe, I. Lunnon, A. Llopis-Pascual, J. Zamecnik, S. Proctor, M. Rodriguez-Frias, M. Turner, A. Lanzon and W. Crowther, "An engineering development of novel hexrotor vehicle for 3D applications", in Proceedings of the International Micro Air Vehicles conference summer edition, 2011, pp. 32-39.

[3] G. Flores, A. Montes de Oca , and A. Flores, "Robust Nonlinear Control for the Fully Actuated Hexa-Rotor: Theory and Experiments," IEEE Control Systems Letters, Vol. 7, 2023

[4] S. Park , J. Lee, J. Ahn, M. Kim, J. Her, G. H. Yang and D. Lee, "ODAR: Aerial Manipulation Platform Enabling Omnidirectional Wrench Generation," IEEE/ASME Transactions On Mechatronics, Vol. 23, No. 4, August 2018.

[5] M. Ryll, H. H. Bulthoff, and P. Robuffo Giordano, Modeling and Control of a Quadrotor UAV with Tilting Propellers, in 2012 IEEE Int. Conf. on Robotics and Automation, 2012.

[6] A. Nemati and M. Kumar, "Modeling and Control of a Single Axis Tilting Quadcopter" in 2014 American Control Conference, 2014.

[7] P. Zheng , X. Tan, B. Bahadir Kocer , E. Yang, and M. Kovac, TiltDrone: A Fully-Actuated Tilting Quadrotor Platform, IEEE Robotics And Automation Letters, Vol. 5, No. 4, October 2020.

[8] E. Cetinsoy, Design and simulation of a holonomic quadrotor UAV with sub-rotor control surfaces, IEEE International Conference on Robotics and Biomimetics (ROBIO), Guangzhou, 2012.

[9] D. Yecheskel, and S. Arogeti, "Modeling and Control of a Hexacopter with a Rotating Seesaw" 14th International Conference on Control, Automation, Robotics Vision, Phuket, 2016 (ICARCV 2016)

[10] S. Bouabdallah, Design and control of quadrotors with application to autonomous flying, PhD dissertation, Lausanne, EPFL, 2007.